nature chemical biology

ARTICLE

PUBLISHED ONLINE: 26 DECEMBER 2010 | DOI: 10.1038/NCHEMBIO.497

Nox2 redox signaling maintains essential cell populations in the brain

Bryan C Dickinson[1], Joseph Peltier[2], Daniel Stone[2], David V Schaffer[2]* & Christopher J Chang[1,3]*

Reactive oxygen species (ROS) are conventionally classified as toxic consequences of aerobic life, and the brain is particularly susceptible to ROS-induced oxidative stress and damage owing to its high energy and oxygen demands. NADPH oxidases (Nox) are a widespread source of brain ROS implicated in seizures, stroke and neurodegeneration. A physiological role for ROS generation in normal brain function has not been established, despite the fact that mice and humans lacking functional Nox proteins have cognitive deficits. Using molecular imaging with Peroxyfluor-6 (PF6), a new selective fluorescent indicator for hydrogen peroxide (H_2O_2), we show that adult hippocampal stem/progenitor cells (AHPs) generate H_2O_2 through Nox2 to regulate intracellular growth signaling pathways, which in turn maintains their normal proliferation *in vitro* and *in vivo*. Our results challenge the traditional view that brain ROS are solely deleterious by demonstrating that controlled ROS chemistry is needed for maintaining specific cell populations.

Oxidative stress from the aberrant accumulation of ROS over time can damage proteins, lipids and nucleic acids[1] and forms the molecular underpinning of the free-radical theory of aging[2]. The brain is particularly sensitive to ROS damage owing to its high oxygen demand and low antioxidant capacity, and oxidative stress is connected to stroke and neurodegenerative diseases for which age is a risk factor[3]. However, the controlled production of ROS occurs throughout development and adult life, presumably for physiological processes, and a major source of brain ROS are the Nox enzymes that are expressed throughout the central nervous system (CNS)[4,5]. These membrane-spanning protein complexes generate H_2O_2 as their final chemical product through the direct two-electron reduction of molecular oxygen by NADPH[5,6] or through one-electron reduction to superoxide (O_2^-) and subsequent conversion to H_2O_2 (refs. 4,5). The established physiological function for Nox proteins is in the immune system, where they participate in phagocytic killing of pathogen invaders[5]. More recently, however, the discovery of Nox enzymes in nonphagocytic cell types throughout the body[6,7] has greatly expanded the scope of potential roles for these complexes, and emerging data link their H_2O_2-producing activity to beneficial cell signaling events[4–15].

The H_2O_2 generated from Nox proteins in the brain and CNS has traditionally been associated with stroke[16], aging[17], seizures[18] and neurodegenerative Alzheimer's[19] and Parkinson's[20] diseases. However, the presence of these proteins in the brain and CNS throughout adult life presages a beneficial role for endogenous ROS production that remains insufficiently understood[21]. Along these lines, both mice and humans that lack functional Nox2 have cognitive deficits[22,23], most notably in learning and memory, suggesting a role for this Nox isoform within the hippocampus. A population of neural stem/progenitor cells resides within the dentate gyrus of the hippocampus and forms new neural tissue in the adult brain that has a role in memory formation[24]. We hypothesized that Nox-generated H_2O_2, which acts as a molecular signal for growth within cultured cell lines[8,9], could help maintain the proliferation of these stem cell populations in the brain.

Here we show that H_2O_2 redox signaling derived from Nox2 is essential for normal growth and proliferation of neural stem cells *in vitro* and *in vivo*. Motivated by the dearth of chemical tools to selectively probe H_2O_2 production in cell types that would not be expected to produce high concentrations of this ROS, we developed Peroxyfluor-6 acetoxymethyl ester (PF6-AM), a new chemoselective fluorescent indicator for H_2O_2 with improved sensitivity. This fluorescent probe features a boronate chemical switch that allows for selective detection of H_2O_2 over other ROS, combined with acetoxymethyl ester–protected phenol and carboxylic acid groups for enhanced cellular retention and sensitivity. After confirming that PF6 is more responsive than previous boronate H_2O_2 reporters, we used this new trappable probe to demonstrate that AHPs produce H_2O_2 when stimulated with fibroblast growth factor-2 (FGF-2), a mitogen that regulates their proliferation[25]. We then show that endogenous H_2O_2 production is important for normal cell signaling through the kinase hub Akt and is mediated by the H_2O_2-producing enzyme Nox2. Moreover, RNA-interference knockdown of Nox2 in cell culture and gene knockout of *Nox2* in mice abrogated normal Akt signaling and AHP function *in vitro* and *in vivo*. Our results highlight the utility of PF6-AM as a tool to help discover new redox chemistry in biological systems and provide evidence that the controlled production of H_2O_2 in the brain can be physiologically beneficial.

RESULTS

Synthesis and evaluation of Peroxyfluor-6

Redox signaling mediated by H_2O_2 has been studied primarily in proliferating cell culture models stimulated with mitogens[9]. As the majority of brain tissue is composed of terminally differentiated cells, we turned our attention to AHPs, which grow and proliferate throughout development and adult life to feed into neuronal and glial populations. Accordingly, we first sought to test whether these neural stem cells produce endogenous H_2O_2 under growth conditions.

Traditional methodologies for imaging H_2O_2 and related ROS in living cells typically use nonspecific indicators that rely on general oxidation and therefore detect an assortment of oxidants[26]. Because neural tissue is highly susceptible to oxidative stress[1,2,21,27], the

[1]Department of Chemistry, University of California, Berkeley, California, USA. [2]Department of Chemical Engineering, University of California, Berkeley, California, USA. [3]Howard Hughes Medical Institute, University of California, Berkeley, California, USA. *e-mail: schaffer@berkeley.edu or chrischang@berkeley.edu

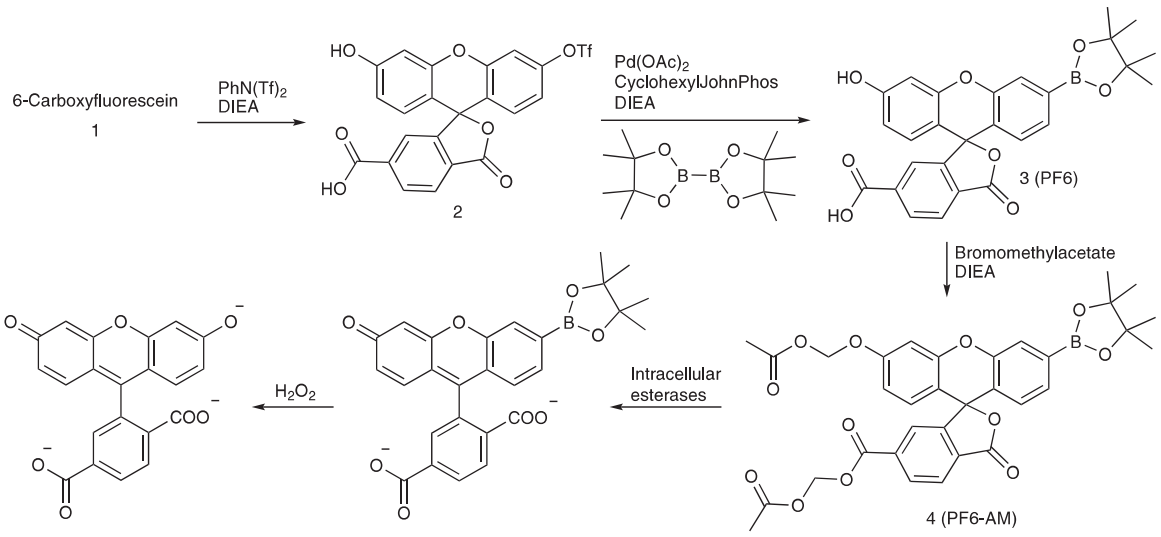

Scheme 1 | Design and synthesis of PF6-AM. DIEA, diisopropylethylamine.

specific ROS that the AHPs come in contact with is a crucial determinant of the ultimate downstream cellular responses. We have shown previously that the conversion of aryl boronates to phenols is a useful chemoselective methodology for the detection of H_2O_2 in biological systems[28]. The first generation of Peroxy dyes, exemplified by PF1 (**Supplementary Fig. 1**), possesses two boronate protecting groups, which, after reaction with two equivalents of H_2O_2, yields fluorescent products[29–32]. This initial work has established that boronate cages offer a general motif for creating fluorescent indicators that can selectively image H_2O_2 over other biologically relevant ROS. Second-generation boronate probes such as Peroxy Green 1 (PG1) and MitoPY1 (**Supplementary Fig. 1**) use a single boronate deprotection to increase sensitivity and allow for detection of H_2O_2 generated in oxidative stress[33], neurodegenerative disease[34,35] and immune[36] and growth-factor signaling models[37,38]. However, these available boronate dyes were not sufficiently sensitive to visualize potential H_2O_2 production in AHPs after stimulation with the endogenous mitogen FGF-2 (**Supplementary Fig. 2**).

We sought to improve the sensitivity of boronate-based probes while maintaining their high selectivity for H_2O_2. Inspired by work showing that increasing cellular retention of fluorescent probes is a practical strategy to improve sensitivity[39–43], we designed and synthesized PF6-AM, a carboxyfluorescein-based probe combining a boronate-masked phenol for H_2O_2 detection and acetoxymethyl ester groups to cap phenol and carboxylic acid functionalities for enhanced cellular retention (**Scheme 1**, **Supplementary Methods**). Briefly, monotriflation of 6-carboxyfluorescein **1** using stoichiometric *N*-phenyl bis(trifluoromethanesulfonamide) affords triflate **2** in 60% yield. Palladium-mediated borylation of **2** with cyclohexyl JohnPhos, bis(pinacolato) diboron and diisopropylethylamine in anhydrous 1,4-dioxane at room temperature provides PF6 **3** in 80% yield. Finally, protection with bromomethyl acetate furnishes acetoxymethyl ester–protected PF6-AM **4**. The lipophilic acetoxymethyl esters allow the probe to pass readily through cell membranes into the cytoplasm, where esterases can then deprotect the acetoxymethyl ester groups to reveal PF6, a dianionic form of the probe that is membrane impermeable and thus trapped inside the cell, where it can respond to changes in intracellular H_2O_2 levels. We reasoned that this trappable probe should have increased sensitivity compared to the previously developed first- and second-generation boronate probes, owing to a combination of greater local concentration of probe substrate retained within cells as well as a slower rate of deprotected probe product leaking out of cells. PF6 features two visible-region absorptions (λ_{abs} = 460 nm, ε = 14,000 M^{-1} cm^{-1}; λ_{abs} = 370 nm, ε = 10,000 M^{-1} cm^{-1}) and a weak emission (λ_{em} = 530 nm, Φ = 0.10). Spectrophotometric studies confirmed that PF6 responds to H_2O_2 by a turn-on fluorescence response and is selective for H_2O_2 over a host of other ROS oxidants (**Fig. 1a**,**b**). Kinetics measurements of the H_2O_2-mediated boronate deprotection were performed under pseudo–first-order conditions (5 μM dye, 10 mM H_2O_2), giving an observed rate constant of $k = 3.3(1) \times 10^{-3}$ s^{-1}.

Validation of PF6 for molecular imaging in cell culture

Having obtained data characterizing the properties and H_2O_2-induced turn-on response of PF6 *in vitro*, we sought to evaluate its utility for molecular imaging in cell culture model systems. First, we assayed whether the acetoxymethyl ester cage groups were sufficient to increase retention of the probe within living cells. We used the boronate-based H_2O_2 probe PG1, which is sensitive to signaling levels of H_2O_2 but does not possess esterase-cleavable groups, as a benchmark for these studies. PG1 and PF6 use the same excitation and emission wavelengths and have similar emission characteristics, allowing for direct comparison of the uptake and retention of these probes in cell culture by scanning confocal microscopy. After loading HeLa cells with either PG1 or PF6-AM, we thoroughly washed away excess dye. The cells were then imaged immediately after washing and visualized again after 10, 30 and 60 min (**Fig. 1c**,**d**). Cells loaded with PG1 showed modest intracellular fluorescence immediately after washing, but the signal dropped off markedly by the 10-min time point. In contrast, cells loaded with PF6-AM showed intracellular fluorescence immediately after washing that was approximately twice as bright as that in PG1-loaded cells, and they maintained this emission intensity throughout the time course of the measurements. A similar trend was observed in analogous experiments using HEK 293 cells (**Supplementary Fig. 3**).

We next established whether this increased cellular uptake and retention would permit PF6 to detect low levels of H_2O_2 in live samples. HeLa cells were loaded with PF6-AM and then stimulated with either 10 μM H_2O_2 or carrier for 30 min (**Fig. 1e**,**f**). Cells treated with H_2O_2 showed greater intracellular fluorescence than control samples, even at this relatively low level of exogenously added H_2O_2. Similar results were seen in HEK 293 cells (**Supplementary Fig. 3**). A drawback to this approach is that the probe is not retained after fixation, making it incompatible with immunostaining in fixed cell and tissue samples. Future synthetic directions include enhancing the photostability of these dyes, adding functional groups that allow for maintenance of the probe upon fixation and expanding the color palette of trappable H_2O_2 probes for multicolor imaging experiments. Nevertheless, these experiments confirm that PF6 is

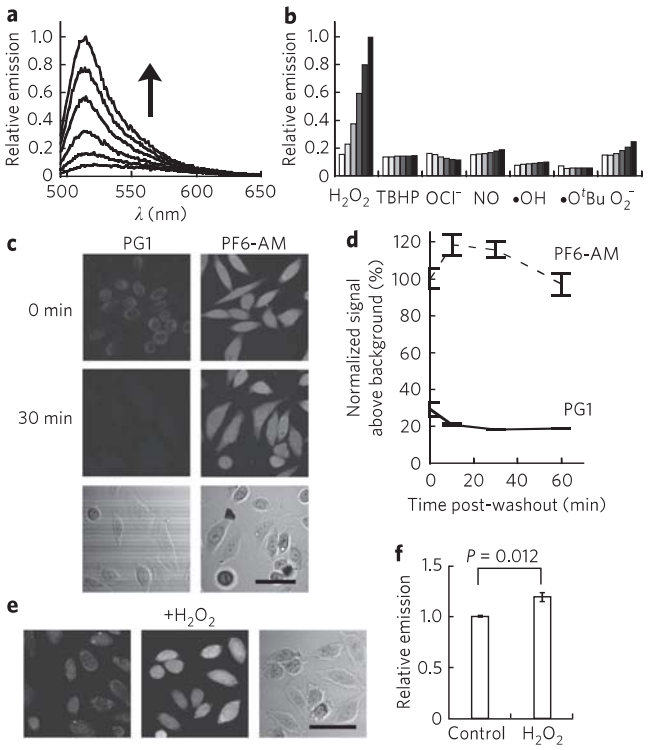

Figure 1 | Spectroscopic characterization and cell culture validation of PF6-AM. (**a**) Fluorescence turn-on response of 5 μM PF6 at 0, 5, 15, 30, 45 and 60 min after the addition of 100 μM H_2O_2. (**b**) Fluorescence responses of 5 μM PF6 to various ROS. Bars represent relative responses at 0, 5, 15, 30, 45 and 60 min after addition of each ROS. Data shown are for 10 mM O_2^- (with 10 μM catalase), 200 μM NO and 100 μM all other ROS. (**c**) Uptake and retention of PF6. HeLa cells were loaded with either 5 μM PG1 or 5 μM PF6-AM for 15 min, then washed twice with DPBS and imaged at 0 or 30 min after dye washing. Images were also captured at 10 and 60 min (not shown). Bright-field images of cells are shown below. Scale bar, 50 μm. (**d**) Quantification of data in **c**. (**e**) Sensitivity of PF6. HeLa cells were loaded with 5 μM PF6-AM for 15 min, stimulated with either water carrier or 10 μM H_2O_2 for 30 min, and imaged. Bright-field image of cells is shown at right. Scale bar, 50 μm. (**f**) Quantification of data in **e**. Statistical analyses were performed with a two-tailed Student's *t*-test; error bars in **d** and **f** show ± s.e.m.

a selective and sensitive reporter for intracellular H_2O_2 in live cells and further validate the strategy of increased cellular uptake and retention as a general method for increasing the sensitivity of small-molecule fluorescent probes. To the arsenal of ROS probes currently available, including those for general oxidants[44] and superoxide[35,45], PF6 adds an H_2O_2-specific fluorescent probe with selectivity and sensitivity to signaling levels of this oxygen metabolite.

PF6 reveals that AHPs produce H_2O_2 upon FGF-2 stimulation

After validating PF6 in model systems, we sought to apply this new tool to the study of AHP cells. To this end, AHPs were isolated from the hippocampi of 6-week-old female Fisher 344 rats as previously described[25]. After fibroblast growth factor 2 (FGF-2) withdrawal, AHPs were loaded with PF6-AM and treated with either FGF-2 mitogen or carrier. Cells stimulated with FGF-2 showed greater intracellular fluorescence than unstimulated control AHPs, as measured by PF6 imaging (**Fig. 2** and **Supplementary Fig. 4**). Toxicity studies showed that PF6-AM is nontoxic at the concentration used in this study (**Supplementary Figs. 5** and **6**). When coupled with the *in vitro* selectivity characterization of PF6, these data indicate that FGF-2 induces the endogenous production of H_2O_2 in AHPs. Furthermore, these data demonstrate the utility of this new chemical tool for detecting changes in low levels of H_2O_2 in live-cell settings. Intrigued at the finding that AHPs, an essential cell population of the CNS from development throughout adult life, produce a compound known to have potential toxic consequences in the brain[46], we next aimed to elucidating potential roles for H_2O_2 in physiological (rather than pathological) processes of these cells.

H_2O_2 is required for growth signaling in AHPs

Having established through molecular imaging that AHPs produce H_2O_2 upon mitogen stimulation, we next probed whether FGF-2–induced H_2O_2 generation could influence downstream cell signaling cascades. In regard to this question, a noteworthy relationship has already emerged between endogenous H_2O_2 production and PI3 kinase (PI3K)-dependent activation of the kinase Akt, a signaling pathway that has several potentially redox-regulated components. For example, previous studies have demonstrated that PTEN, a phosphatase that opposes forward PI3K signaling, contains a catalytic active site residue, Cys124, that is reversibly oxidized by H_2O_2 to form a disulfide with Cys71. This oxidative redox switch turns off the activity of the phosphatase, allowing the PI3K-Akt signaling cascade to propagate forward; re-reduction of this disulfide to the corresponding thiols restores PTEN phosphatase activity, resetting the cycle[47]. The PI3K-dependent activation of Akt is crucial for the growth and proliferation of AHPs, as in previous studies, either pharmacological inhibition of Akt or the expression of a dominant-negative Akt inhibited AHP proliferation[48]. Accordingly, we first investigated the effects of exogenous H_2O_2 addition to AHPs by monitoring the phosphorylation status of Akt.

Toxicity studies demonstrated that AHPs can withstand H_2O_2 to notably high concentrations for short periods of time (**Supplementary Fig. 7**). Treatment of AHPs with H_2O_2 in the absence of FGF-2 stimulation was sufficient to trigger a marked dose-dependent increase in phospho-Akt, without increasing the phosphorylation status of another major signaling hub, the MAP kinases ERK1 and ERK2 (**Fig. 3a** and **Supplementary Fig. 8**). Previous work has shown that pharmacological inhibition of the ERK1/2 MAP kinase pathway does not strongly affect AHP proliferation[48].

We then investigated the effect of endogenously produced H_2O_2 on the phosphorylation status of Akt. FGF-2 stimulation of AHPs triggered a time-dependent increase in the phosphorylation of Akt compared to control samples. In contrast, cells expressing catalase, an enzyme that quickly destroys H_2O_2, had diminished FGF-2–induced phosphorylation of Akt (**Fig. 3b**) and produced less H_2O_2 as detected by PF6-AM imaging (**Fig. 2b** and **Supplementary Fig. 4**). Additionally, pretreatment with the general antioxidant *N*-acetylcysteine (NAC), which quenches H_2O_2, or with the flavin and Nox inhibitor diphenyleneiodonium (DPI), which inhibits most potential intracellular sources of H_2O_2, both blocked the FGF-2–induced phosphorylation of Akt, as well as affected the phosphorylation of ERK1 and ERK2 to a lesser extent (**Fig. 3c**). To confirm that DPI at this concentration concomitantly blocks the H_2O_2 signal and Akt phosphorylation, we observed that pretreatment of PF6-AM–loaded AHPs with DPI abolished FGF-2–induced H_2O_2 production (**Fig. 2a** and **Supplementary Fig. 4**).

These experiments demonstrate that AHPs use redox chemistry to modulate this growth-signaling kinase pathway. We then attempted to identify potential targets of the H_2O_2 along the Akt pathway. We used a methodology for assaying the oxidation status of PTEN that relies on differences in gel mobility between the oxidized, disulfide form and the reduced form of the protein[49] to demonstrate that FGF-2 stimulation does indeed produce a small but detectable amount of oxidized PTEN (**Supplementary Fig. 9**). However, this approach toward assaying the oxidation state of PTEN is not very sensitive or consistent in this system, which is why we

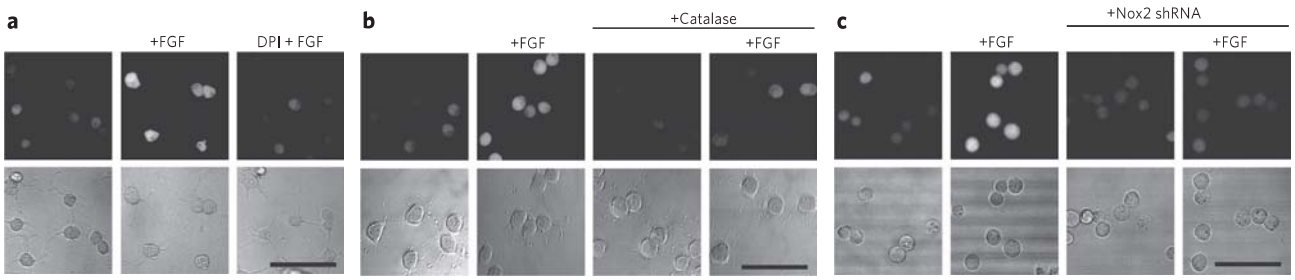

Figure 2 | Application of PF6 to demonstrate that AHPs produce H_2O_2 upon FGF-2 stimulation. (**a**) After FGF-2 starvation, AHPs were loaded with 5 μM PF6-AM for 30 min, stimulated with 20 ng ml^{-1} FGF-2 or media for 30 min, and then imaged. For DPI treatment, cells were preincubated in medium containing 5 μM DPI before FGF-2 stimulation. (**b**) AHPs were transfected with either catalase vector or control vector and treated as in **a**. (**c**) AHPs were transfected with either Nox2 shRNA vector or control vector and treated as in **a**. In **a**–**c**, bright-field images are shown below each representative fluorescent image; scale bars, 50 μm.

continued to monitor Akt phosphorylation, a much more reliable readout of redox signaling, in subsequent experiments.

Nox2 is the source of H_2O_2-mediated signaling in AHPs

We next sought to determine the molecular source of the redox signal within the AHPs. Given the vast expression of Nox2 in the CNS[21], we looked to this protein as a potential redox modulator in AHPs. Both reverse-transcription PCR (RT-PCR; **Fig. 3d**) and western blot analysis using two separate Nox2 antibodies, from rabbit and from mouse (**Fig. 3e**), confirmed the presence of Nox2 in AHPs. Both antibodies produced a band at the same molecular weight, corresponding to the approximate molecular weight of Nox2 (~65 kDa), whose intensity selectively decreased upon genetic manipulation with Nox2-targeted short hairpin RNA (shRNA). The mouse antibody produced a nonspecific band slightly below the Nox2 band that did not change upon treatment with Nox2 shRNA; this band can therefore serve as a loading control.

We used genetic manipulation of Nox2, as well as the fluorescent signal measured with PF6-AM, to investigate the contributions of Nox2 to Akt signaling pathways. AHPs transfected with Nox2-targeted shRNA showed lower Nox2 protein levels and less FGF-2–induced phosphorylation of Akt compared to control cells transfected with an empty vector (**Fig. 3f**). As was observed with chemical inhibition by NAC or DPI, the ERK1 and ERK2 pathway in AHPs also seems to be affected by the lack of Nox2. In addition, AHPs transfected with Nox2-targeted shRNA showed less H_2O_2 production in response to FGF-2 stimulation (**Fig. 2c** and **Supplementary Fig. 4**).

As a further validation of the shRNA knockdown experiments, we designed and tested another shRNA construct targeting an alternative member of the Nox family, Nox3. Nox2 shRNA–transfected cells showed reduced levels of Nox2 compared to Nox3 shRNA–transfected cells and concomitantly showed less response to FGF-2–induced phospho-Akt production (**Fig. 3g**), confirming the specificity of the Nox2 shRNA effects. Together, these data demonstrate that Nox2-generated H_2O_2 contributes to the regulation of growth-signaling pathways within the AHPs.

Nox2 is required for normal AHP proliferation *in vitro*

Having established that intracellular redox changes affect signaling at the protein level, we then sought to determine whether decreased

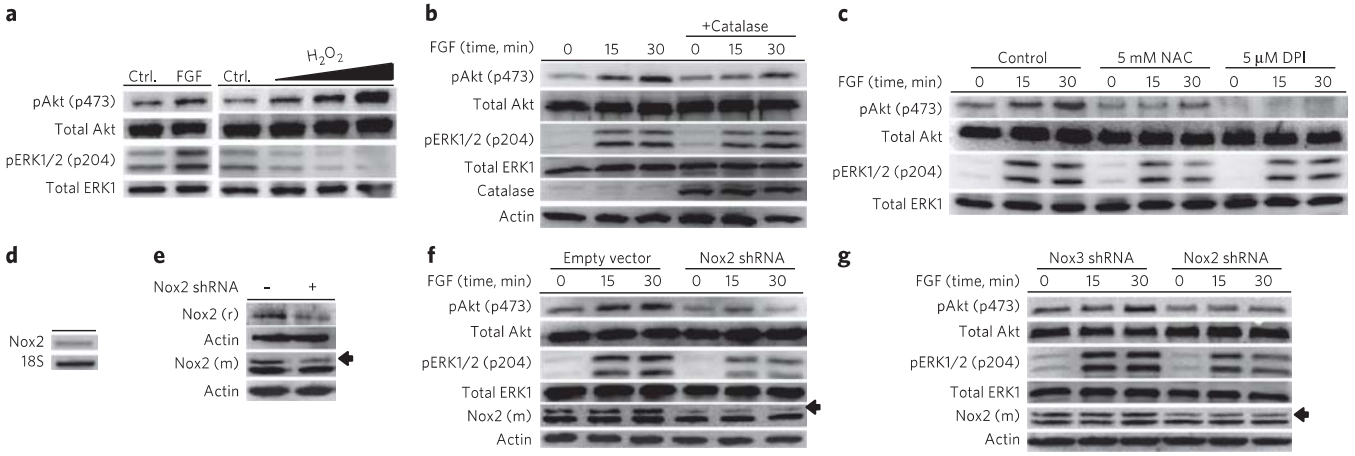

Figure 3 | Cellular redox status affects AHP growth signaling. (**a**–**c**) Western blots showing phosphorylated (p) and total Akt and ERK1/2. In **a**, after FGF-2 starvation, AHPs were stimulated with vehicle control (Ctrl.), with 20 ng ml^{-1} FGF-2, or with 300, 500 or 1,000 μM H_2O_2 (wedge indicates increasing doses) for 30 min. In **b**, AHPs were transfected with either catalase vector or a control vector. After FGF-2 starvation, AHPs were stimulated with 20 ng ml^{-1} FGF-2 and lysed at the indicated time points. In **c**, After FGF-2 starvation, AHPs were incubated with NAC, DPI or vehicle control (DMSO) for 40 min, then stimulated with 20 ng ml^{-1} FGF-2 and lysed at the indicated time points. (**d**) Nox2 mRNA detection in AHPs measured by RT-PCR. 18S rRNA was used as a loading control. (**e**) Nox2 expression of AHP whole-cell extracts transfected with either Nox2 shRNA or an empty vector, measured by western blot analysis using either a mouse monoclonal (m) or a rabbit polyclonal (r) Nox2 antibody, and stripped and reprobed for actin as a loading control. Arrow marks the band in the Nox2 monoclonal antibody blot that matches the band in the Nox2 polyclonal blot and corresponds to the molecular weight of Nox2. (**f**,**g**) Western blots from AHPs transfected with either empty vector, Nox2 shRNA or Nox3 shRNA. After 12 h FGF-2 starvation, AHPs were stimulated with 20 ng ml^{-1} FGF-2 and lysed at the indicated time points. phospho-Akt, phospho-ERK and Nox2 were analyzed from whole-cell extracts, and blots were stripped and reprobed for total protein or actin as loading controls.

redox signaling would also produce similar results in functional assays. We therefore investigated the effects of diminished redox signaling on AHP proliferation in the presence of FGF-2. First, 5-d *in vitro* proliferation experiments were performed in the presence of varying levels of DPI. We observed a dose-dependent decrease in growth rate with DPI inhibition, with concentrations as low as 50 nM having an inhibitory effect (**Fig. 4a**). As DPI is relatively nonspecific and will block all flavin-containing sources of ROS, we sought to elucidate the role of Nox2 specifically. We therefore transfected AHPs with shRNA constructs targeting Nox2 or the empty vector. In agreement with the chemical inhibition experiments and western blot analysis, the Nox2 shRNA–transfected cells showed a slower proliferation rate than that of AHPs containing the empty vector (**Fig. 4b**) or that of cells expressing Nox3 shRNA as a control (**Fig. 4c**). Together, these data indicate that FGF-2 signaling involves the production of H_2O_2 through the activation of Nox2, which influences signaling through Akt and ultimately the downstream phenotype of growth rate.

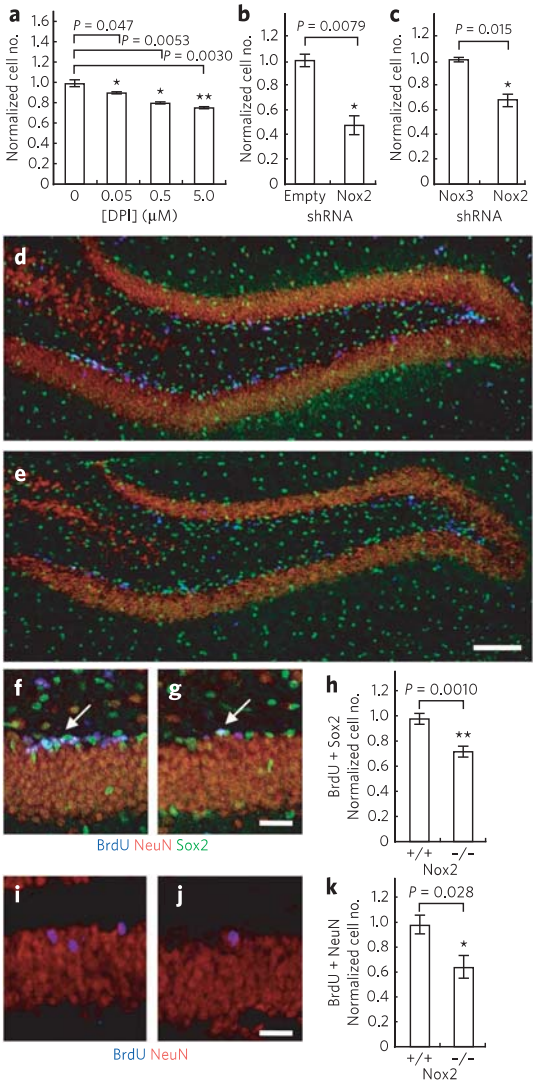

Figure 4 | Nox2 is essential for normal proliferation of AHPs *in vitro* and *in vivo*. (**a**) Results from 5-day growth assay of AHPs grown in the presence of FGF-2 and varying concentrations of DPI ($n = 4$). (**b**) Results from 5-day growth assay of AHPs transfected with either Nox2 shRNA or the empty vector and grown in the presence of FGF-2 ($n = 3$). (**c**) Results from 5-day growth assay of AHPs transfected with either Nox2 shRNA or Nox3 shRNA and grown in the presence of FGF-2 ($n = 3$). (**d**,**e**) Dentate gyrus of a CL57BL/6J mouse (**d**) and a *Nox2*$^{-/-}$ mouse (**e**) after 7 d of BrdU injections. Scale bar, 100 μm. (**f**,**g**) Examples of a cluster of AHPs positive for BrdU and Sox2 in a CL57BL/6J control mouse (**f**) and of a single BrdU- and Sox2-positive cell in a *Nox2*$^{-/-}$ mouse (**g**), after 7 d of BrdU injections. Scale bar, 20 μm. Sections were stained for BrdU (blue), NeuN (red) and Sox2 (green). (**h**) Quantification of BrdU- and Sox2-positive cells in either control or *Nox2*$^{-/-}$ mice after 7 d of BrdU injections ($n = 5$). (**i**,**j**) Example of newborn neurons in a CL57BL/6J control mouse (**i**) and in a *Nox2*$^{-/-}$ mouse (**j**) 28 d after 7 d of BrdU injections. Scale bar, 20 μm. (**k**) Quantification of BrdU- and NeuN-positive cells in either control or *Nox2*$^{-/-}$ mice 28 d after 7 d of BrdU injections ($n = 4$). For all graphs, data were normalized to controls and statistical analyses were performed with a two-tailed Student's *t*-test; $^*P \leq 0.05$; $^{**}P \leq 0.005$; and error bars show ± s.e.m.

Nox2 is required for normal AHP function *in vivo*

We then sought to extend these *in vitro* findings to an *in vivo* system. To this end, we performed bromodeoxyuridine (BrdU) incorporation experiments in Nox2 knockout (*Nox2*$^{-/-}$) mice and CL57BL/6J control mice. BrdU incorporates into the genomes of dividing cells and can then be detected by immunohistochemistry after fixation, along with stem cell or neuronal markers. Therefore, cells that stain for both BrdU as well as a stem cell marker are AHPs that proliferated during the course of the injections. Mice were injected with BrdU daily for 7 d and perfused 24 h after the final injection. Immunohistochemical assessments of the dentate gyri from *Nox2*$^{-/-}$ and control mice showed no morphological abnormalities (**Fig. 4d**,**e**), suggesting that the dentate gyrus develops normally in the *Nox2*$^{-/-}$ mice. However, quantification of the proliferating AHP populations on the basis of colocalization of BrdU and Sox2, a stem cell marker[50], revealed a marked decrease in the number of proliferating AHPs in the *Nox2*$^{-/-}$ mice (**Fig. 4f–h**), establishing that Nox2 contributes to the normal proliferation of AHPs *in vivo*.

Finally, we assayed the effects of Nox2 deficiency on adult neurogenesis *in vivo*. For these experiments, mice were injected with BrdU daily for 7 d and were then perfused 28 d after the final injection. The brains were then analyzed for cells that stained for both BrdU and NeuN, a neuronal marker, which would indicate neurons that had differentiated from AHPs within the time course of the experiment. Quantification of the colocalization of BrdU and NeuN revealed a reduction in the number of newborn neurons in the *Nox2*$^{-/-}$ mice (**Fig. 4i–k**), establishing that Nox2 also contributes to adult neurogenesis *in vivo*.

DISCUSSION

H_2O_2 is emerging as a newly recognized messenger for cell signaling, and a major source of peroxide produced through stimulation of various cell-surface receptors is the Nox family of proteins[5,9,10,26]. These ROS-generating enzymes are classically associated with phagocytic cells during immune responses, in which they are used to combat pathogens by attacking them with controlled oxidative bursts. More recent results have revealed the widespread distribution of Nox complexes in nonphagocytic cell types throughout the body[5], implying that H_2O_2 generation is physiologically necessary; however, many aspects of how and why this small-molecule oxidant is required and used for the benefit of living organisms remain elusive. To address these questions, we developed a new H_2O_2-specific fluorescent probe, PF6, and applied this new chemical tool to demonstrate that AHPs, an essential population of cells that proliferate in the brain from development throughout adult life, respond to growth conditions by producing H_2O_2. Through a combination of imaging, pharmacological and genetic experiments, we have revealed that Nox2-mediated H_2O_2 production is important for maintaining normal signaling and proliferation of AHPs *in vitro*. Moreover, we show that mice lacking functional Nox2 have fewer proliferating neural stem cells and less adult neurogenesis in the

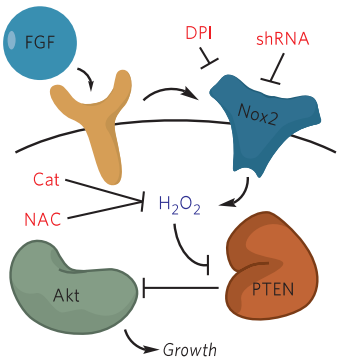

Figure 5 | Model for the role of Nox2 in FGF-2 redox signaling in AHPs. The mitogen FGF-2 induces the production of H_2O_2 in AHPs, which can be blocked by either the general flavin inhibitor DPI, the antioxidant NAC, the expression of catalase (Cat) or genetic manipulation of Nox2. Nox2-generated H_2O_2 oxidizes and deactivates PTEN, which enhances signaling through Akt and alters growth rates of AHPs *in vitro* and *in vivo*.

hippocampus, which establishes that H_2O_2-mediated redox signaling is essential on the whole-organism scale.

The collective data provide a molecular model for the cognitive deficits observed in mice and humans lacking the ROS-generating Nox2 enzyme (**Fig. 5**) and establish that ROS are not exclusively detrimental to brain tissue, despite their harmful effects in the context of seizures, stroke and neurodegeneration. As various isoforms of the Nox family are present throughout the brain and CNS[4], there are probably many other beneficial roles for these ROS-producing proteins in this system. Indeed, the *in vivo* effects observed in the *Nox2*-knockout mice could also be influenced by a lack of Nox2 in other cell types within brain. In a broader sense, our findings show that controlled ROS production and signaling can be used as a strategy for maintaining proliferation of essential cell populations in the body. Finally, these results suggest caution when applying antioxidant therapeutics in a nonspecific fashion, as ROS production can be a necessary component for the fitness of a given system.

METHODS

6-Carboxyfluorescein monotriflate (2). 6-Carboxyfluorescein (512 mg, 1.36 mmol) was dissolved in 15 ml of 2:1 acetonitrile/dimethyl formamide. Diisopropylethylamine (2.2 ml, 13.3 mmol) was then added and the reaction stirred for 10 min. *N*-Phenyl bis(trifluoromethanesulfonamide) (487 mg, 1.36 mmol) was then added and the reaction was stirred overnight at room temperature. The reaction mixture was then dried under reduced pressure. Purification by column chromatography (19:1 dichloromethane/methanol) afforded compound **5** as a yellow oil (412 mg, 60% yield). ^{1}H NMR ($CDCl_3$/10% CD_3OD, 400 MHz): δ 8.26 (1H, d, J = 8.0 Hz), 8.02 (1H, d, J = 8.2 Hz), 7.77 (1H, s), 7.19 (1H, d, J = 2.4 Hz), 6.90 (1H, dd, J = 2.4, 8.8 Hz), 6.82 (1H, d, J = 8.8 Hz), 6.76 (1H, d, J = 2.4 Hz), 6.59 (1H, dd, J = 2.4, 8.8 Hz), 6.54 (1H, d, J = 8.8Hz). ^{13}C NMR ($CDCl_3$/10% CD_3OD, 100 MHz): δ 168.6, 159.8, 152.5, 152.1, 151.8, 150.0, 138.4, 131.5, 130.0, 129.1, 128.9, 125.3, 125.1, 119.2, 116.5, 113.4, 110.5, 108.5, 103.0, 82.5. ^{19}F NMR ($CDCl_3$/10% CD_3OD, 376.5 MHz): δ –71.97. HR-FABMS: calculated for [M$^+$] 509.0149, found 509.0158.

PF6 and PF6-AM (3 and 4). Compound **2** (412 mg, 0.81 mmol), $Pd(OAc)_2$ (55 mg, 0.081 mmol), bis(pinacolato)diboron (308 mg, 1.22 mmol), cyclohexyl JohnPhos (114 mg, 0.32 mmol), diisopropylethylamine (594 mg, 4.63 mmol) and 5 ml dioxane were added to a vial in an inert-atmosphere glove box and the reaction was stirred overnight at room temperature. The vial was then removed from the glove box and the contents were evaporated to dryness. Purification by column chromatography (19:1 dichloromethane/methanol) furnished PF6 as a yellow solid (317 mg, 80% yield). ^{1}H NMR ($CDCl_3$/5% CD_3OD, 400 MHz): δ 8.26 (1H, d, J = 8.0 Hz), 8.06 (1H, d, J = 8.0 Hz), 7.78 (1H, s), 7.71 (1H, s), 7.39 (1H, d, J = 8.0 Hz), 6.72–6.76 (2H, m), 6.58 (1H, d, J = 8.8 Hz), 6.53 (1H, dd, J = 2.4, 8.8 Hz), 1.32 (12H, s). ^{13}C NMR ($CDCl_3$/10% CD_3OD, 100 MHz): δ 169.1, 167.5, 159.1, 153.5, 152.3, 150.7, 136.9, 131.3, 129.7, 129.2, 129.0, 127.1, 125.5, 125.1, 123.6, 120.7, 112.6, 109.2, 103.1, 20.7. HR-FABMS: calculated for [M$^+$] 487.1559, found 487.1567. PF6 (40 mg, 0.08 mmol), bromomethyl acetate (51 mg, 0.33 mmol), diisopropylethylamine (32 mg, 0.25 mmol) and 1 ml dimethyl formamide were stirred at room temperature overnight. The reaction mixture was then extracted into dichloromethane, washed three times with water, washed once with brine, dried over magnesium sulfate and dried under reduced pressure. Purification by column chromatography (7:3 ethyl acetate/hexanes) produced PF6-AM as a white solid (11 mg, 22% yield). ^{1}H NMR ($(CD_3)_2O$, 500 MHz): δ 7.99-8.06 (1H, m), 7.81 (1H, t, J = 6.0 Hz), 7.72–7.79 (1H, m), 7.66 (1H, s), 7.43–7.50 (1H, m), 7.26–7.31 (1H, m), 6.97–7.10 (1H, m), 6.87–6.95 (1H, m), 6.81–6.88 (1H, m), 5.30–6.00 (4H, m), 2.01–2.11 (6H, m), 1.34 (12H, m). HR-FABMS: calculated for [M$^+$] 631.1981, found 631.1979.

Cell culture. AHPs were cultured on tissue-culture polystyrene coated with poly-ornithine and 5 μg ml^{-1} of laminin (Invitrogen), and grown in DMEM/F-12 (1:1) high-glucose medium (Invitrogen) containing N-2 supplement (Invitrogen) and 20 ng ml^{-1} recombinant human FGF-2 (Peprotech). For FGF-2 starvation, AHPs were washed once with DMEM/F-12 (1:1) high-glucose medium, and then placed in DMEM/F-12 (1:1) high-glucose medium without FGF-2 for 12–16 h.

AHP fluorescence imaging experiments. Confocal fluorescence imaging studies on AHPS were performed with a Zeiss LSM510 NLO Axiovert 200 laser scanning inverted microscope and a ×40 oil-immersion objective lens. Excitation of PF6-AM–loaded AHPs at 488 nm was carried out with an argon laser and emission was collected using a 500- to 550-nm filter set. AHPs were incubated with 5 μM PF6-AM in DMEM/F12 (1:1) with N-2 supplement for 30 min at 37 °C. The cells were then washed twice with fresh DMEM/F12 plus N-2, incubated in DMEM/F12 plus N-2, either with or without 20 ng ml^{-1} FGF-2 for 30 min, and then imaged. For the DPI-inhibited cells, 5 μM DPI was included in the media for all incubations. Images were analyzed in ImageJ (Wayne Rasband, US National Institutes of Health, http://rsbweb.nih.gov/ij/) with at least ten cells counted per field in four separate fields for each condition.

Received 16 March 2010; accepted 18 October 2010; published online 26 December 2010

References

1. Floyd, R.A. Oxidative damage to behavior during aging. *Science* **254**, 1597 (1991).
2. Harman, D. The aging process. *Proc. Natl. Acad. Sci. USA* **78**, 7124–7128 (1981).
3. Andersen, J.K. Oxidative stress in neurodegeneration: cause or consequence? *Nat. Med.* **10**, S18–S25 (2004).
4. Bedard, K. & Krause, K.H. The NOX family of ROS-generating NADPH oxidases: physiology and pathophysiology. *Physiol. Rev.* **87**, 245–313 (2007).
5. Lambeth, J.D. NOX enzymes and the biology of reactive oxygen. *Nat. Rev. Immunol.* **4**, 181–189 (2004).
6. Geiszt, M., Kopp, J.B., Várnai, P. & Leto, T.L. Identification of renox, an NAD(P)H oxidase in kidney. *Proc. Natl. Acad. Sci. USA* **97**, 8010–8014 (2000).
7. Suh, Y.A. *et al.* Cell transformation by the superoxide-generating oxidase Mox1. *Nature* **401**, 79–82 (1999).
8. Sundaresan, M., Yu, Z.X., Ferrans, V.J., Irani, K. & Finkel, T. Requirement for generation of H2O2 for platelet-derived growth factor signal transduction. *Science* **270**, 296–299 (1995).
9. Rhee, S.G. H2O2, a necessary evil for cell signaling. *Science* **312**, 1882–1883 (2006).
10. D'Autréaux, B. & Toledano, M.B. ROS as signalling molecules: mechanisms that generate specificity in ROS homeostasis. *Nat. Rev. Mol. Cell Biol.* **8**, 813–824 (2007).
11. Poole, L.B. & Nelson, K.J. Discovering mechanisms of signaling-mediated cysteine oxidation. *Curr. Opin. Chem. Biol.* **12**, 18–24 (2008).
12. Woo, H.A. *et al.* Inactivation of peroxiredoxin I by phosphorylation allows localized H2O2 accumulation for cell signaling. *Cell* **140**, 517–528 (2010).
13. Niethammer, P., Grabher, C., Look, A.T. & Mitchison, T.J. A tissue-scale gradient of hydrogen peroxide mediates rapid wound detection in zebrafish. *Nature* **459**, 996–999 (2009).
14. Paulsen, C.E. & Carroll, K.S. Orchestrating redox signaling networks through regulatory cysteine switches. *ACS Chem. Biol.* **5**, 47–62 (2010).
15. Miller, E.W., Dickinson, B.C. & Chang, C.J. Aquaporin-3 mediates hydrogen peroxide uptake to regulate downstream intracellular signaling. *Proc. Natl. Acad. Sci. USA* **107**, 15681–15686 (2010).
16. Walder, C.E. *et al.* Ischemic stroke injury is reduced in mice lacking a functional NADPH oxidase. *Stroke* **28**, 2252–2258 (1997).
17. Park, L., Anrather, J., Girouard, H., Zhou, P. & Iadecola, C. Nox2-derived reactive oxygen species mediate neurovascular dysregulation in the aging mouse brain. *J. Cereb. Blood Flow Metab.* **27**, 1908–1918 (2007).
18. Behrens, M.M. *et al.* Ketamine-induced loss of phenotype of fast-spiking interneurons is mediated by NADPH-oxidase. *Science* **318**, 1645–1647 (2007).
19. Park, L. *et al.* Nox2-derived radicals contribute to neurovascular and behavioral dysfunction in mice overexpressing the amyloid precursor protein. *Proc. Natl. Acad. Sci. USA* **105**, 1347–1352 (2008).

20. Zhang, W. *et al.* Neuroprotective effect of dextromethorphan in the MPTP Parkinson's disease model: role of NADPH oxidase. *FASEB J.* **18**, 589–591 (2004).
21. Sorce, S. & Krause, K.H. NOX enzymes in the central nervous system: from signaling to disease. *Antioxid. Redox Signal.* **11**, 2481–2504 (2009).
22. Pao, M. *et al.* Cognitive function in patients with Chronic Granulomatous Disease: a preliminary report. *Psychosomatics* **45**, 230–234 (2004).
23. Kishida, K.T. *et al.* Synaptic plasticity deficits and mild memory impairments in mouse models of chronic granulomatous disease. *Mol. Cell. Biol.* **26**, 5908–5920 (2006).
24. Zhao, C., Deng, W. & Gage, F.H. Mechanisms and functional implications of adult neurogenesis. *Cell* **132**, 645–660 (2008).
25. Palmer, T.D., Markakis, E.A., Willhoite, A.R., Safar, F. & Gage, F.H. Fibroblast growth factor-2 activates a latent neurogenic program in neural stem cells from diverse regions of the adult CNS. *J. Neurosci.* **19**, 8487–8497 (1999).
26. Winterbourn, C.C. Reconciling the chemistry and biology of reactive oxygen species. *Nat. Chem. Biol.* **4**, 278–286 (2008).
27. Barnham, K.J., Masters, C.L. & Bush, A.I. Neurodegenerative diseases and oxidative stress. *Nat. Rev. Drug Discov.* **3**, 205–214 (2004).
28. Miller, E.W. & Chang, C.J. Fluorescent probes for nitric oxide and hydrogen peroxide in cell signaling. *Curr. Opin. Chem. Biol.* **11**, 620–625 (2007).
29. Chang, M.C.Y., Pralle, A., Isacoff, E.Y. & Chang, C.J. A selective, cell-permeable optical probe for hydrogen peroxide in living cells. *J. Am. Chem. Soc.* **126**, 15392–15393 (2004).
30. Miller, E.W., Albers, A.E., Pralle, A., Isacoff, E.Y. & Chang, C.J. Boronate-based fluorescent probes for imaging cellular hydrogen peroxide. *J. Am. Chem. Soc.* **127**, 16652–16659 (2005).
31. Albers, A.E., Okreglak, V.S. & Chang, C.J. A FRET-based approach to ratiometric fluorescence detection of hydrogen peroxide. *J. Am. Chem. Soc.* **128**, 9640–9641 (2006).
32. Albers, A.E., Dickinson, B.C., Miller, E.W. & Chang, C.J. A red-emitting naphthofluorescein-based fluorescent probe for selective detection of hydrogen peroxide in living cells. *Bioorg. Med. Chem. Lett.* **18**, 5948–5950 (2008).
33. Srikun, D., Albers, A.E., Nam, C.I., Ivarone, A.T. & Chang, C.J. Organelle-targetable fluorescent probes for imaging hydrogen peroxide in living cells via SNAP-tag protein labeling. *J. Am. Chem. Soc.* **132**, 4455–4465 (2010).
34. Dickinson, B.C. & Chang, C.J. A targetable fluorescent probe for imaging hydrogen peroxide in the mitochondria of living cells. *J. Am. Chem. Soc.* **130**, 9638–9639 (2008).
35. Dickinson, B.C., Srikun, D. & Chang, C.J. Mitochondrial-targeted fluorescent probes for reactive oxygen species. *Curr. Opin. Chem. Biol.* **14**, 50–56 (2010).
36. Srikun, D., Miller, E.W., Domaille, D.W. & Chang, C.J. An ICT-based approach to ratiometric fluorescence imaging of hydrogen peroxide produced in living cells. *J. Am. Chem. Soc.* **130**, 4596–4597 (2008).
37. Miller, E.W., Tulyathan, O., Isacoff, E.Y. & Chang, C.J. Molecular imaging of hydrogen peroxide produced for cell signaling. *Nat. Chem. Biol.* **3**, 263–267 (2007).
38. Dickinson, B.C., Huynh, C. & Chang, C.J. A palette of fluorescent probes with varying emission colors for imaging hydrogen peroxide signaling in living cells. *J. Am. Chem. Soc.* **132**, 5906–5915 (2010).
39. Tsien, R.Y. A non-disruptive technique for loading calcium buffers and indicators into cells. *Nature* **290**, 527–528 (1981).
40. Izumi, S., Urano, Y., Hanaoka, K., Terai, T. & Nagano, T. A simple and effective strategy to increase the sensitivity of fluorescence probes in living cells. *J. Am. Chem. Soc.* **131**, 10189–10200 (2009).
41. Pluth, M.D., McQuade, L.E. & Lippard, S.J. Cell-trappable fluorescent probes for nitric oxide visualization in living cells. *Org. Lett.* **12**, 2318–2321 (2010).
42. McQuade, L.E. & Lippard, S.J. Cell-trappable quinoline-derivatized fluoresceins for selective and reversible biological Zn(ii) detection. *Inorg. Chem.* **49**, 9535–9545 (2010).
43. McQuade, L.E. *et al.* Visualization of nitric oxide production in the mouse main olfactory bulb by a cell-trappable copper(II) fluorescent probe. *Proc. Natl. Acad. Sci. USA* **107**, 8525–8530 (2010).
44. Hempel, S.L., Buettner, G.R., O'Malley, Y.Q., Wessels, D.A. & Flaherty, D.M. Dihydrofluorescein diacetate is superior for detecting intracellular oxidants: comparison with 2′,7′-dichlorodihydrofluorescein diacetate, 5(and 6)-carboxy-2′,7′-dichlorodihydrofluorescein diacetate, and dihydrorhodamine 123. *Free Radic. Biol. Med.* **27**, 146–159 (1999).
45. Robinson, K.M. *et al.* Selective fluorescent imaging of superoxide in vivo using ethidium-based probes. *Proc. Natl. Acad. Sci. USA* **103**, 15038–15043 (2006).
46. Prozorovski, T. *et al.* Sirt1 contributes critically to the redox-dependent fate of neural progenitors. *Nat. Cell Biol.* **10**, 385–394 (2008).
47. Kwon, J. *et al.* Reversible oxidation and inactivation of the tumor suppressor PTEN in cells stimulated with peptide growth factors. *Proc. Natl. Acad. Sci. USA* **101**, 16419–16424 (2004).
48. Peltier, J., O'Neill, A. & Schaffer, D.V. PI3K/Akt and CREB regulate adult neural hippocampal progenitor proliferation and differentiation. *Dev. Neurobiol.* **67**, 1348–1361 (2007).
49. Lee, S.R. *et al.* Reversible inactivation of the tumor suppressor PTEN by H2O2. *J. Biol. Chem.* **277**, 20336–20342 (2002).
50. Suh, H. *et al.* In vivo fate analysis reveals the multipotent and self-renewal capacities of Sox2+ neural stem cells in the adult hippocampus. *Cell Stem Cell* **1**, 515–528 (2007).

Acknowledgments

We thank the Packard and Sloan Foundations (C.J.C.), the UC Berkeley Hellman Faculty Fund (C.J.C.), Amgen, Astra Zeneca and Novartis (C.J.C.) and the US National Institutes of Health (GM 79465 to C.J.C. and EB 007295 to D.V.S.) for providing funding for this work. C.J.C. is an Investigator with the Howard Hughes Medical Institute. B.C.D. was partially supported by a Chemical Biology Training Grant from the US National Institutes of Health. (T32 GM066698). J.P. was partially supported by a training grant fellowship from the California Institute for Regenerative Medicine (T1-00007). We thank M. Quinn (Montana State University) for generous donation of Nox2 antibodies and T. Kawahara for helpful advice.

Author contributions

B.C.D. synthesized all compounds in the paper and performed all analytical measurements, imaging assays and cell culture and mouse experiments. J.P. collaborated on cell culture, RT-PCR and mouse experiments. D.S. helped with mouse experiments. C.J.C., D.V.S., B.C.D. and J.P. designed experimental strategies. C.J.C. and B.C.D. wrote the paper with input from all coauthors.

Competing financial interests

The authors declare no competing financial interests.

Additional information

Supplementary information and chemical compound information is available online at http://www.nature.com/naturechemicalbiology/. Reprints and permissions information is available online at http://npg.nature.com/reprintsandpermissions/. Correspondence and requests for materials should be addressed to D.V.S. or C.J.C.